Prolonged dexamethasone exposure enhances zebrafish lateral-line regeneration but disrupts mitochondrial homeostasis and hair cell function

Allison L. Saettele[1], Hiu-tung C Wong[2], Katie S Kindt[2], Mark E Warchol[1,3] and Lavinia Sheets*[1,4]

1. Department of Otolaryngology, Washington University School of Medicine, St. Louis, MO, USA
2. Section on Sensory Cell Development and Function, National Institutes on Deafness and Other Communication Disorders, National Institutes of Health, Bethesda, USA
3. Department of Neuroscience, Washington University School of Medicine, St. Louis, MO, USA
4. Department of Developmental Biology, Washington University School of Medicine, St. Louis, MO, USA

*** Corresponding author**

Lavinia Sheets: sheetsl@wustl.edu

ORCID ID

HTC Wong : 0000-0001-5826-8526

KS Kindt: 0000-0002-1065-8215

ME Warchol: 0000-0002-0445-6318

L Sheets: 0000-0001-5231-2450

Keywords: neuromast, regeneration, dexamethasone, mitochondrial homeostasis

Abstract

The synthetic glucocorticoid dexamethasone is commonly used to treat inner ear disorders. Previous work in larval zebrafish has shown that dexamethasone treatment enhances hair cell regeneration, yet dexamethasone has also been shown to inhibit regeneration of peripheral nerves after lesion. We therefore used the zebrafish model to determine the impact of dexamethasone treatment on lateral-line hair cells and primary afferents. To explore dexamethasone in the context of regeneration, we used copper sulfate ($CuSO_4$) to induce hair cell loss and retraction of nerve terminals, and then allowed animals to recover in dexamethasone for 48 hours. Consistent with previously work, we observed significantly more regenerated hair cells in dexamethasone-treated larvae. Importantly, we found that the afferent processes beneath neuromasts also regenerated in the presence of dexamethasone and formed an appropriate number of synapses, indicating that innervation of hair cells was not inhibited by dexamethasone. In addition to regeneration, we also explored the effects of prolonged dexamethasone exposure on lateral-line homeostasis and function. Following dexamethasone treatment, we observed hyperpolarized mitochondrial membrane potentials ($\Delta\Psi m$) in neuromast hair cells and supporting cells. Hair cells exposed to dexamethasone were also more vulnerable to neomycin-induced cell death. In response to a fluid-jet delivered

saturating stimulus, calcium influx through hair cell mechanotransduction channels was significantly reduced, yet presynaptic calcium influx was unchanged. Cumulatively, these observations indicate that dexamethasone enhances hair cell regeneration in lateral-line neuromasts, yet also disrupts mitochondrial homeostasis, making hair cells more vulnerable to ototoxic insults and possibly impacting hair cell function.

Introduction

Glucocorticoids are the major hormones of the stress response pathway. Through interactions with ubiquitously expressed receptors, glucocorticoids are involved in regulating many physiological processes, including circadian cycle, tissue homeostasis, metabolism, and inflammation (Vettorazzi et al., 2021). Synthetic glucocorticoids, such as dexamethasone, are commonly used to treat inner ear disorders, such as sudden hearing loss and Menier's disease, and have been proposed as an intervention to protect against cisplatin ototoxicity (Waissbluth et al., 2013). Achieving therapeutic levels of synthetic glucocorticoids in the inner ear with systemic oral delivery of the drug requires high-dose therapy associated with adverse side effects (Egli Gallo et al., 2013). Furthermore, systemic delivery of glucocorticoids to prevent cisplatin ototoxicity may render some types of malignant cells insensitive to cisplatin chemotherapy (Ge et al., 2012). Consequently, local intratympanic delivery directly into the ear has been tested as a potential method for the prevention and treatment of inner ear disease (Marshak et al., 2014; Patel, 2017). One limitation to this approach is that dexamethasone is rapidly cleared from the middle ear (Salt et al., 2011). Thus, strategies to provide sustained delivery of dexamethasone to the inner ear are an active area of research (Fernandez et al., 2016; Liao et al., 2021). While retention of synthetic glucocorticoids in the ear may provide greater therapeutic benefits, the effects of prolonged dexamethasone exposure on hair cell organ homeostasis and function are not well defined.

The zebrafish model has been used in numerous studies evaluating the effects of dexamethasone exposure on biological processes, including wound repair and complex tissue regeneration. In a previous study, dexamethasone was identified in a large-scale screen as an enhancer of hair cell regeneration after neomycin damage to zebrafish lateral-line organs, as well as inducing the addition of hair cells to lateral-line neuromasts in the absence of damage (Namdaran et al., 2012). By contrast, treatment with dexamethasone has been shown to inhibit peripheral nerve and spinal motor nerve regeneration in zebrafish (Bremer et al., 2017; Ohnmacht et al., 2016). Cumulatively, these data suggest that, while dexamethasone potentiates the generation of lateral-line hair cells, reinnervation of dexamethasone-induced hair cells may be impaired.

68 In this study we sought to address two questions: 1) does dexamethasone treatment
69 enhance or inhibit afferent innervation and synapse formation in regenerating lateral-line
70 organs, and 2) does prolonged dexamethasone exposure affect hair cell homeostasis and
71 function? Our results reveal that dexamethasone treatment does not inhibit either afferent
72 innervation or synapse formation in newly produced hair cells. However, dexamethasone
73 treatment does increase mitochondrial activity in existing hair cells and reduces their evoked
74 mechanosensory responses, suggesting that prolonged dexamethasone exposure may
75 adversely affect hair cell function.

76 Materials and Methods

77 *Ethics statement*

78 Experimental procedures were performed with approval from the Washington University
79 School of Medicine or NIH Institutional Animal Care and Use Committee, and in accordance
80 with NIH guidelines for use of zebrafish.

81 *Zebrafish*

82 Adult zebrafish were raised under standard conditions at 27-29°C in the Washington
83 University or NIH Zebrafish Facility. Embryos were raised in incubators at 28°C in embryo
84 media (EM; 15 mM NaCl, 0.5 mM KCl, 1 mM $CaCl_2$, 1 mM $MgSO_4$, 0.15 mM KH_2PO_4, 0.042 mM
85 Na_2HPO_4, 0.714 mM $NaHCO_3$) with a 14 h:10 h light:dark cycle. At 3-4 days post fertilization
86 (dpf), larvae were anesthetized in 0.02% tricaine methanesulfonate (MS-222) and screened for
87 transgenic fluorophores using a Leica MZ10 F stereomicroscope with fluorescence equipped
88 with a GFP and a DSR filter set. After screening, 4 dpf, larvae were raised in 100-200 ml EM
89 media in 250-ml plastic beakers and fed rotifers daily. Sex of the animal was not considered for
90 this study because sex cannot be determined in larval zebrafish.

91 *Transgenic lines*

92 The following transgenic lines were used in this study: nl1Tg *(TgBAC(neurod1:EGFP))*
93 (Obholzer et al., 2008) ; w78Tg (*Tg(myo6b:GCaMP3))* and w119Tg (*Tg(myo6b:mitoGCaMP3))*
94 (Esterberg et al., 2013), w200Tg *(Tg(mpeg1:yfp))* (Roca & Ramakrishnan, 2013), y229Gt
95 *(Tg(tnks1bp1:EGFP))* (Behra et al., 2012) and idc1Tg (*Tg(myo6b:GCaMP6sCAAX))* (Sheets et
96 al., 2017).

97 *Copper ablation of neuromasts and dexamethasone post-treatment*

98 To ablate lateral-line neuromast hair cells and induce afferent neurite retraction, 5 dpf
99 larvae were exposed to 3 μM $CuSO_4$ (Sigma-Aldrich, Cat# 451677) diluted in EM in cell

100 strainers (Corning; Cat# 431752) for 1 hour. This concentration and time course
101 of $CuSO_4$ exposure was verified as the optimal minimum dose to induce complete neuromast
102 hair cell loss (mean hair cell number per neuromast: 11 ± 3 (control) vs 0 ± 1 (3 uM $CuSO_4$), 14
103 fish per condition, 3 trials). After exposure, larvae were rinsed, and then allowed to swim freely
104 during a 2-hour recovery in EM. Immediately following this 2-hour recovery, larvae were moved
105 to 6-well plates (Falcon, Cat# 351146) containing 4 mL EM per well with either 0.1% DMSO
106 (drug carrier alone) or 0.1% DMSO + 10 μM dexamethasone (Sigma-Aldrich, Cat# D1756) for
107 48 hours. The dexamethasone concentration used in this study (10 μM) was based on the
108 concentration used in a previous study that identified dexamethasone as an enhancer of lateral-
109 line hair cell regeneration (Namdaran et al., 2012). Larvae were maintained at 28ºC throughout
110 $CuSO_4$ exposure and dexamethasone post-treatments.

111 *Neomycin ablation of neuromasts with dexamethasone pre-treatment*

112 Macrophages are effector cells of the innate immune system, and in a previous study we
113 observed robust recruitment of macrophages to neomycin-injured neuromasts (Warchol et al.,
114 2021). To test whether dexamethasone treatment inhibited macrophage recruitment following
115 hair cell injury, 5 dpf w200Tg *(Tg(mpeg1:yfp))* larvae were pre-treated with 0.1% DMSO or 1-50
116 μM dexamethasone in EM for 24 hours. Following pre-treatment, larvae were rinsed twice and
117 placed in cell strainers, and then exposed to 100 μM neomycin (Sigma-Aldrich, Cat# N1876) for
118 30 minutes. Following neomycin exposure, fish were rinsed and moved to 6-well plates with 4
119 mL of EM to recover for 1 hour. Exposure and recovery times for neomycin treatment were
120 chosen based on previous studies evaluating aminoglycoside toxicity in zebrafish lateral-line
121 hair cells (Coffin et al., 2013; Owens et al., 2009).

122 To test whether dexamethasone pre-treatment sensitized hair cells to ototoxic insults, 5
123 dpf wild-type larvae were pre-treated with 0.1% DMSO or 10 μM for 48 hours, then exposed to
124 0-100 μM neomycin as described above.

125 *Whole-mount Immunohistochemistry*

126 Free-swimming larvae were exposed to DAPI (1:2000, 4 minutes; D3571, Thermo
127 Fisher) to label hair cell nuclei, then sedated on ice for 4 min. For GFP immunolabeling to label
128 the afferent process or for Otoferlin immunolabeling to label hair cells, larvae were fixed (4%
129 paraformaldehyde, 4% sucrose, 150 μM $CaCl_2$, 0.1 M phosphate buffer) in 2 mL Eppendorf
130 tubes overnight at 4-8°C. For synaptic labeling, larvae were fixed for 5 hours at 4-8°C.

131 Larvae fixed overnight were blocked in phosphate-buffered saline (PBS: 8 g NaCl, 0.2 g
132 KCl, 0.24 g KH_2PO_4, 14.4 g Na_2HPO_4 per 1 L distilled H_2O) with 5% normal horse serum (NHS;

133 Sigma-Aldrich, Cat# H0146), 1% DMSO, 1% Triton X-100 (Sigma-Aldrich, Cat# T8787) for 2
134 hours at room temperature. Primary antibody exposure was performed in PBS with 2% NHS,
135 0.1% Triton-X100. Secondary antibody exposure was performed in PBS with 2% NHS.
136 Following all antibody exposures, larvae were rinsed several times in PBS with 0.1% Tween-20
137 (Sigma-Aldrich, Cat# P9416).

138 For synaptic labeling, larvae were fixed for 5 hours, permeabilized in ice-cold acetone (-
139 20°C, 5 min, Sigma-Aldrich, Cat# 179124), then blocked in PBS with 2% goat serum (Sigma-
140 Aldrich, Cat# G9023), 1% bovine serum albumin (BSA; Sigma-Aldrich, Cat# A9647), and 1%
141 DMSO for 2 hours. Primary and secondary antibody solutions and all post-antibody rinses were
142 performed in the same PBS, BSA, and DMSO concentration mix used for blocking.

143 Primary antibodies:

144 - Mouse IgG2a α-CtBP (1:2000; Santa Cruz Biotech, Inc; Cat#: sc-55502)
145 - Mouse IgG1 α-MAGUK (K28/86; 1:500; NeuroMab, UC Davis; Cat# 75-029)
146 - Chicken α-GFP (1:500; Aves Labs, Inc; Cat# GFP-1020)
147 - Mouse IgG2a α-Otoferlin (1:500; Developmental Studies Hybridoma Bank; HCS-
148 1)

149 Secondary antibodies (used at 1:1000):

150 - Goat α-chicken (Alexa 488) - neurites
151 - Goat α-mouse IgG1 (Alexa 488) – MAGUK
152 - Goat α-mouse IgG1 (Alexa 647) - MAGUK
153 - Goat α-mouse IgG2a (Alexa 647) - CtBP
154 - Goat α-mouse IgG2a (DyLight 550/Alexa546) – CtBP

155 All fish were rinsed in PBS prior to being mounted on glass slides in elvanol (13% w/v
156 polyvinyl alcohol, 33% w/v glycerol, 1% w/v DABCO (1,4 diazobicylo[2,2,2] octane) in 0.2 M
157 Tris, pH 8.5) and #1.5 cover slips.

158 *FM1-43 labeling:*

159 To evaluate hair cell mechanotransduction (Toro et al., 2015), 7dpf larvae were
160 anesthetized in EM containing 0.01% Tricaine (EMT), exposed to 3 μM FM1-43 (N-(3-
161 triethylammoniumpropyl)-4-(4-(dibutylamino)-styryl) pyridinium dibromide; ThermoFisher, Cat#
162 T3163) for 20 seconds, rinsed in EMT, and then mounted on a FluoroDish (World Precision
163 Instruments, Inc., Cat# FD3510) in low-melt agarose (Invitrogen, Cat# 16520) containing 0.01%
164 Tricaine (LMAT). The agarose was allowed 2.5 minutes to solidify before covering in EMT and
165 imaging.

166 *TMRE labeling*

167 To measure mitochondrial ΔΨm, y229Gt *(Tg(tnks1bp1:EGFP))* transgenic larvae were
168 exposed to 250 nM tetramethylrhodamine ethyl ester perchlorate (TMRE, Thermo Fisher, Cat#
169 T669) diluted in EM for 25 minutes while wrapped in foil, then rinsed, allowed to equilibrate for
170 10-15 minutes, and mounted on a FluoroDish in LMAT. The agarose was allowed 2.5 minutes to
171 solidify before covering in EMT and imaging.

172 *Confocal imaging*

173 Most confocal images were acquired via an ORCA-Flash 4.0 V3 camera (Hamamatsu)
174 using a Leica DM6 Fixed Stage microscope with an X-Light V2TP spinning disc confocal (60
175 micron pinholes) equipped with an LDI-7 laser diode illuminator (89 North). Image acquisition
176 was controlled by MetaMorph software. *For fixed imaging:* z-stack images ~10-15 µm depth with
177 a z-step of 0.2 µm were acquired using a 63x/1.4 N.A. oil immersion objective. *For live imaging:*
178 larvae were anesthetized with 0.01% tricaine in EM, then mounted lateral-side up on a thin layer
179 of 1% low-melt agarose in a tissue culture dish with a cover-glass bottom (FluoroDish; World
180 Precision Instruments) and covered in EMT media. Z-stack images of neuromast L3-5 were
181 acquired with a 63x/0.9 N.A. water immersion objective. Z- acquisition parameters with X-light
182 spinning disc: z step of 1 µm, laser "20% power" for all wavelengths, 100 ms per frame for fixed
183 imaging, 120 ms per frame for live imaging. Images in Fig. 5 were acquired using an LSM 700
184 laser scanning confocal microscope with a 63x 1.4 NA Plan-Apochromat oil-immersion objective
185 (Carl Zeiss). Confocal z-stacks of ~15 µm depth were acquired with a z-step of 1 µm.

186 *Confocal image processing and analysis*

187 Fiji (ImageJ software) was used to process and analyze most confocal images
188 (Schneider et al., 2012). To analyze macrophage activation and inflammation, confocal images
189 were reconstructed and analyzed using Volocity software (Quorum Technologies). Subsequent
190 image processing for display within figures was performed using Illustrator software (Adobe).
191 Hair cell counts were quantified from hair cell specific DAPI labeled nuclei or from cells
192 immunolabeled for Otoferlin (HCS-1; Fig. 5). To quantify hair cell synapses, raw images
193 containing single immunolabel were converted to 8-bit, then subtracted for background using a
194 20-pixel (CtBP) or 10-pixel (MAGUK) rolling ball radius. Puncta were defined as regions of
195 immunolabel with pixel intensity above a determined threshold: threshold for Ribeye label was
196 calculated using the Isodata algorithm and threshold for MAGUK label was calculated using the
197 Yen algorithm. Intact synapses were defined as CtBP immunolabel juxtaposed with MAGUK
198 and quantified by scrolling through image z-stacks.

199 To measure neurite length, the ImageJ plugin Simple Neurite Tracer (Longair et al.,
200 2011) was used on z-stack images of GFP-labeled afferent neurons. Following ImageJ's Basic
201 Instructions, which can be found in the Help drop-down menu of the Tracer plugin, neurites
202 were traced by scrolling through the z-stack and creating paths. All neurite structures making up
203 the basket-like processes that surround the neuromast were included in the paths, as well as
204 the stalk at the base of the neuromast where innervating neurites emerged from the main
205 afferent neuronal tract and any meandering projections coming off the dendritic basket. The
206 Simple Neurite Tracer automatically detected the path set between two designated points and
207 calculated a measured length in microns. Any branches emerging from and between paths were
208 measured as separate paths. Once fully traced, all paths within the dendritic basket were then
209 added together to get the total neurite length within the neuromast.
210 Macrophage density was quantified by scrolling through image z-stacks and counting the
211 number of macrophages within 25 μm radius of a neuromast (using a circle inscribed on the
212 neuromast). The number of macrophages contacting a neuromast was determined by scrolling
213 through the x-y planes of each image stack (1 μm interval between x-y planes, 15 μm total
214 depth) and counting macrophages that were in direct contact with Otoferlin-labeled hair cells.
215 Finally, the number of macrophages that had internalized Otoferlin-immunolabeled material (hair
216 cell debris) was counted and assumed to reflect the number of phagocytic events. For each
217 metric, the recorded number reflected the activity of a single macrophage, i.e., a macrophage
218 that made contacts with multiple hair cells and/or had internalized debris from several hair cells
219 was still classified as a single 'event.'
220 To measure the baseline fluorescence intensity of indicators across whole neuromasts,
221 images containing single channels were background-subtracted using a rolling ball radius of the
222 following sizes: images containing cytoGCaMp3 or mitoGCaMP3 (50-pixel), images containing
223 FM1-43FX or TMRE label (100-pixel). Whole neuromasts were delineated based on hair cell
224 specific DAPI label in maximum-intensity projections, and mean intensity of the indicator was
225 measured. Measurements from each experimental trial were normalized to the control median
226 value. To accommodate nested data and ensure statistical rigor, we preformed subsequent
227 statistical analysis on average value of measurements from multiple neuromasts (L3, L4, L5)
228 within an individual fish, such that each fish provided a single data point.

229 *Functional calcium imaging*

230 GCaMP6s-based calcium imaging was used to examine evoked signals in zebrafish hair
231 bundles and presynapses, as described previously (Lukasz & Kindt, 2018). Briefly, after 48-hour
232 dexamethasone treatment, individual 7 dpf larvae were first anesthetized with EMT. Pins were

233 used to restrain larvae onto a Sylgard-filled recording chamber. To suppress the movement,
234 alpha-bungarotoxin (125 μM, Tocris) was injected into the cavity of the heart. Larvae were then
235 immersed in extracellular imaging solution (in mM: 140 NaCl, 2 KCl, 2 $CaCl_2$, 1 $MgCl_2$ and 10
236 HEPES, pH 7.3, OSM 310 +/- 10) without tricaine. A fluid jet was used to mechanically stimulate
237 hair bundles (L1-L4) with posterior fluid-flow for 500 ms.

238 To detect evoked calcium responses, images were acquired using a Bruker Swept-field
239 confocal microscope (Bruker Inc), with a Nikon CFI Fluor 60x 1.0 NA water-immersion objective.
240 A Rolera EM-C2 CCD camera (QImaging) was used to detect signals. To measure
241 GCaMP6sCAAX signals, images were acquired with 2x2 binning using a 35 μm slit at 10 Hz in
242 z-stacks of 5 planes every 2 μm or 0.5 μm for presynaptic and hair bundle measurements. High
243 speed imaging along the z-axis was accomplished by using a piezoelectric motor (PICMA P-
244 882.11–888.11 series, Physik Instrumente GmbH). Sequential evoked GCaMP6sCAAX
245 acquisitions were separated by at least 5 min.

246 To quantify the magnitude of evoked GCaMP6s signals, images were processed in FIJI.
247 Z-stacks were max-projected, and images at each timepoint were aligned using StackReg
248 (Thevenaz et al., 1998). A 5 μm and 1.31 μm diameter circular ROI was drawn over each hair
249 cell base and hair bundle respectively to make intensity measurements. To plot evoked changes
250 in GCaMP6s intensity, the baseline (F_0, signal during the 2 s pre-stimulus period) was used to
251 plot the relative change in fluorescent signal from baseline ($\Delta F/F_0$). The magnitude of evoked
252 calcium signals was determined using $\Delta F/F_0$ plots. The baseline GCaMP6s signal F_0 was used
253 to estimate the resting calcium levels in each hair bundle or presynaptic region. The response
254 magnitudes or resting GCaMP6s levels for each neuromast were averaged to obtain a single
255 point per neuromast.

256 *Statistical analysis*

257 Statistical analyses were performed using Prism 9 (Graphpad Software Inc). Datasets
258 were confirmed for normality using the D'Agostino-Pearson test—all the datasets in this study
259 were normally distributed. Statistical significance between two groups was determined by an
260 unpaired Student's t-test if the two populations had the same variance, or an unpaired Welch's
261 unequal variance t-test if the two populations did not have the same variance. Statistical
262 significance between multiple groups with normal distributions was determined by one-way
263 ANOVA and appropriate post-hoc tests. For datasets dependent on multiple independent
264 variables, statistical significance was determined using two-way ANOVA and appropriate post-
265 hoc tests.

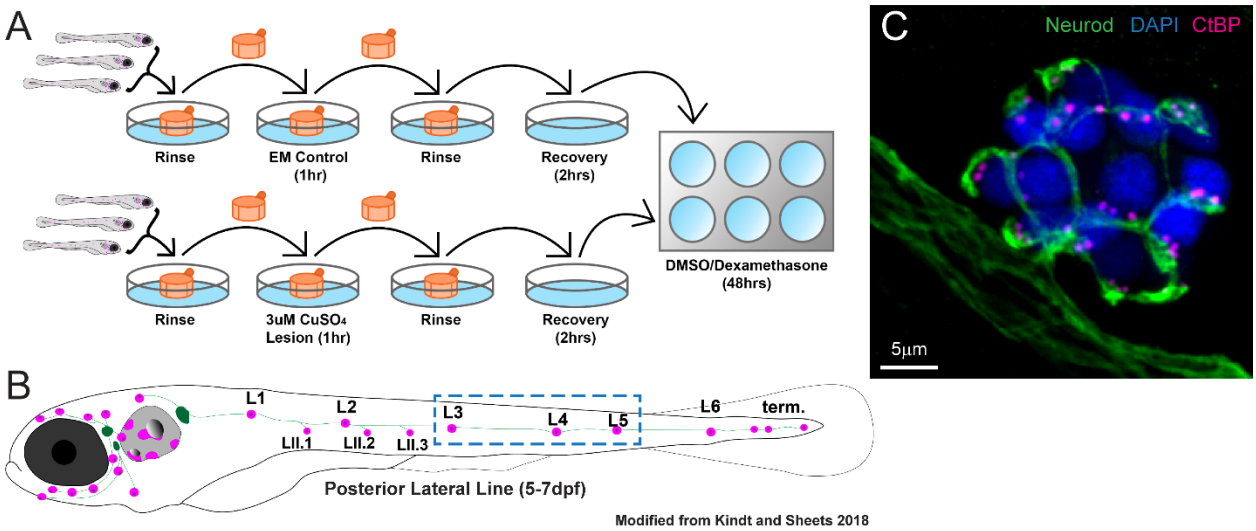

Figure 1. Workflow of $CuSO_4$ lateral-line lesion and dexamethasone exposure
(A) Diagram of workflow for CuSO4 lesions and dexamethasone exposure. Larvae (5 dpf) were placed into cell strainers and moved between rinse and lesion steps, while being allowed to swim freely during recovery and dexamethasone exposure. (B) Diagram of a 5-7dpf zebrafish larvae showing the distribution of lateral line neuromasts (magenta) and innervating afferent nerves (green). This study focused on neuromasts L3, L4, and L5 (blue dashed-line box). (C) Representative maximum intensity projection of confocal z-stack image of neuromast L4 in a 7 dpf zebrafish larvae. Labels: afferent neurons labeled with GFP (green; tgBAC(neurod1:GFP), DAPI-labeled hair-cell nuclei (blue), and immunolabeled presynaptic ribbons (magenta; pan-CtBP).

Results

Dexamethasone enhances regeneration and reinnervation of neuromast hair cells following $CuSO_4$ lesion.

In two separate small molecule screens using zebrafish larvae, dexamethasone has been identified as an enhancer of hair cell regeneration in lateral-line neuromasts and an inhibitor of peripheral fin nerve regeneration (Bremer et al., 2017; Namdaran et al., 2012). Dexamethasone has also been reported to enhance axon regeneration in rats, following injury (Feng & Yuan, 2015). We therefore addressed whether dexamethasone influences afferent reinnervation and hair cell synapse regeneration in zebrafish lateral-line neuromasts. To induce injury, we exposed animals to copper sulfate ($CuSO_4$), which induces loss of lateral-line hair cells and considerable retraction of afferent nerve terminals (Hardy et al., 2021; Mackenzie & Raible, 2012; Olivari et al., 2008). Five-day old zebrafish larvae were treated in either 3 µM $CuSO_4$ in embryo media (EM) or EM alone for 1 hour. After $CuSO_4$ exposure, the animals were allowed to recover for 2 hours, and then transferred to EM containing either 10 µM dexamethasone or drug carrier alone (0.1% DMSO) for 48 hours (Fig. 1A). After 48 hours we assessed the extent of afferent reinnervation and hair cell and synapse regeneration. We focused on posterior lateral-line neuromasts L3-L5 for analysis (Fig. 1B). To examine afferent reinnervation and hair cell regeneration we visualized afferent nerve fibers labeled with GFP as

well as hair cell nuclei labeled with DAPI (Fig. 1C). In agreement with previous observations of lateral-line organs injured with neomycin, we observed a significantly greater number of regenerated hair cells per neuromast in larvae exposed to dexamethasone during regeneration compared to controls (Fig. 2 C-E; orange points, ****adjusted P<0.0001; Tukey's multiple comparisons test). Additionally, among fish that were not exposed to $CuSO_4$ (unlesioned), significantly more hair cells per neuromast were observed in fish that were exposed to dexamethasone (Fig. 2 A,B,E; gray points). This observed increase in hair cell number per neuromast has been previously shown to be due to increased proliferation of hair cell precursors rather than prevention of hair cell turnover (Namdaran et al., 2012). These results therefore confirm that dexamethasone enhances hair cell regeneration and stimulates hair cell precursors to divide, even in the absence of injury.

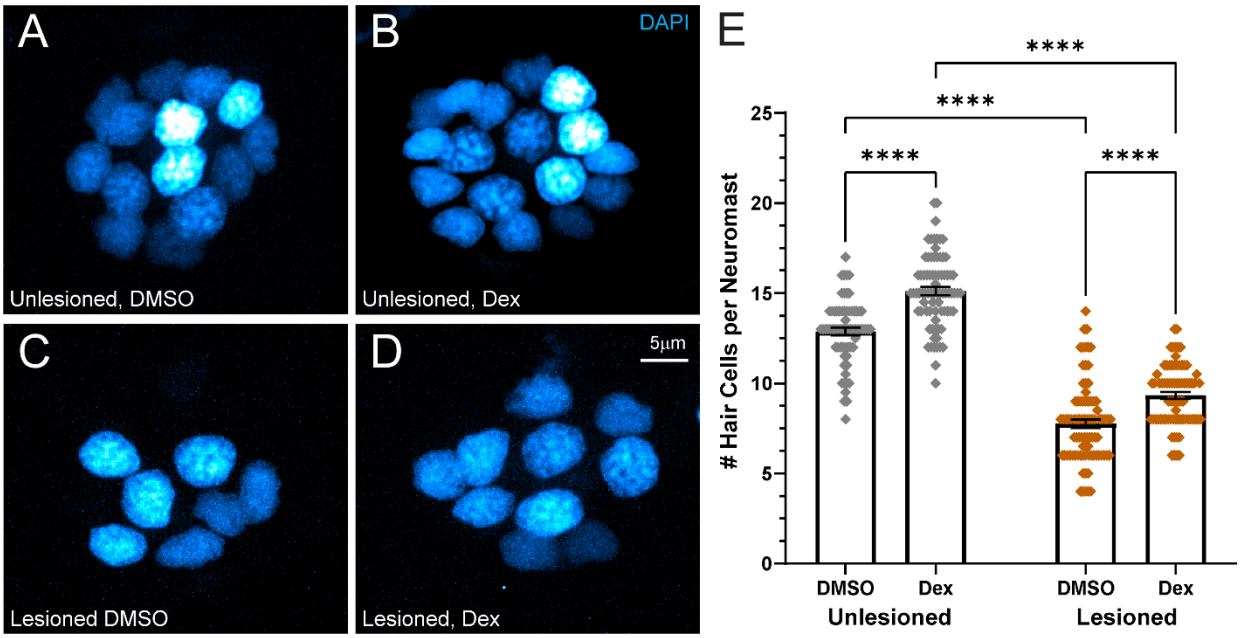

Figure 2. Dexamethasone increased hair cell number in intact and regenerating neuromasts
(A-D) Representative maximum intensity projection images of 7dpf neuromasts, with DAPI-labeled hair cell nuclei (blue). Larval lateral line neuromasts were either left intact (unlesioned) (A, B) or lesioned by treatment with 3µM $CuSO_4$ for 1 hour (C, D). Larvae were then allowed to recover for 2hrs, then exposed for 48 hr to either 0.1% DMSO (carrier) (A, C) or dexamethasone (B, D). (E) Scatter plot graph of hair cell number per neuromast. Bars indicate mean and SEM. Each dot represents a single neuromast on an individual fish. Both intact (unlesioned) and regenerating neuromasts showed a significant increase in the number of hair cells per neuromast in dexamethasone-treated fish relative to DMSO controls (****adjusted P<0.0001). N= 5-10 fish per condition per trial; 7 experimental trials.

To determine whether dexamethasone treatment enhanced or inhibited afferent innervation of hair cells, we measured the length of innervating afferent processes in both unlesioned and lesioned neuromast after regeneration (Fig. 3 A-D). In neuromasts that had regenerated after $CuSO_4$-induced lesions, we observed that the average length of afferent

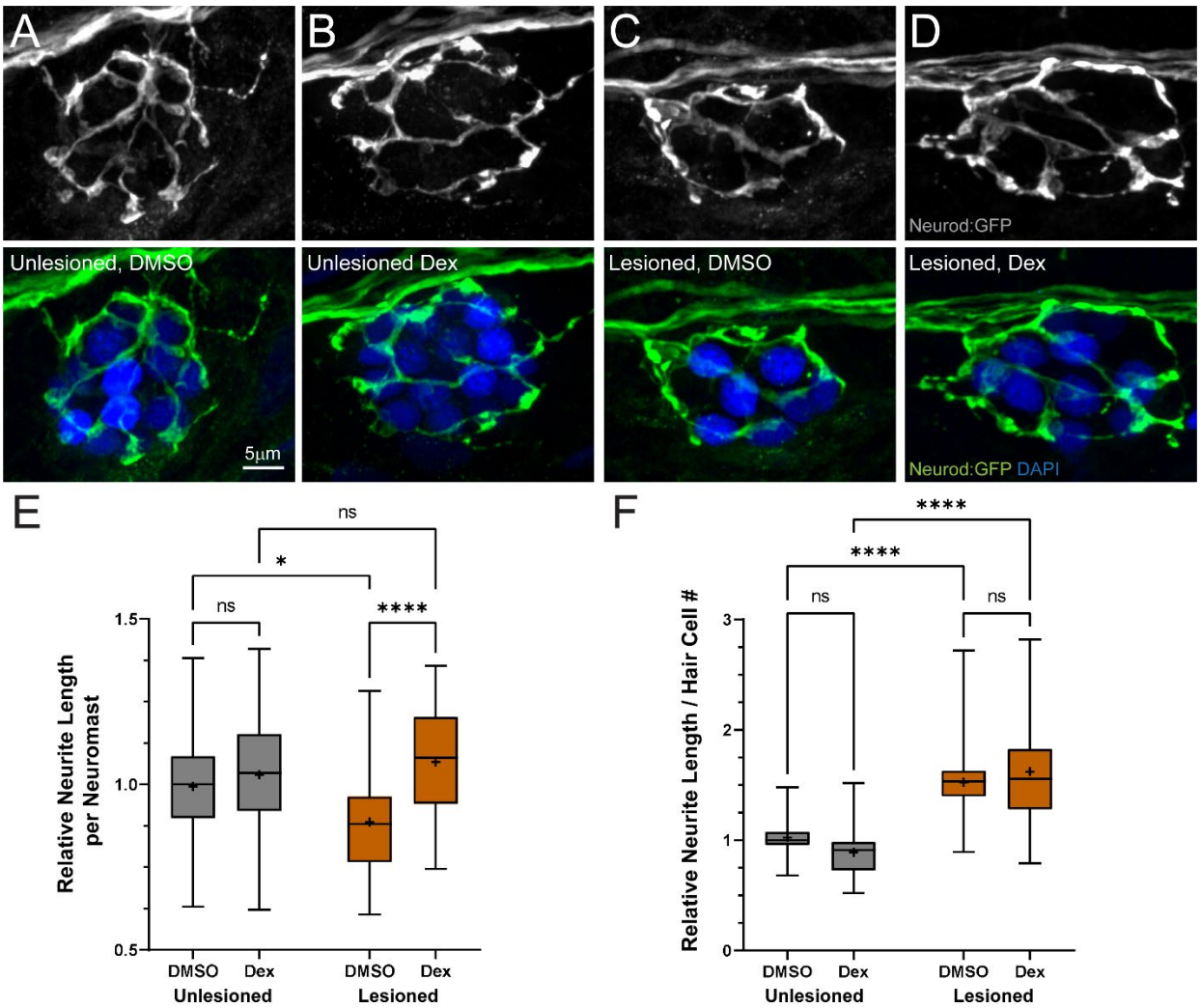

Figure 3. Dexamethasone enhanced afferent innervation of regenerating neuromasts
(A-D) Representative maximum intensity projection images of pLL neuromasts in 7dpf tgBAC(neurod1:GFP) larvae showing afferent neurons (green) and DAPI-labeled hair-cell nuclei (blue). Neuromasts were either unlesioned (A, B) or lesioned with $CuSO_4$ (C, D), then allowed to regenerate for 48 hr while exposed to DMSO (carrier) (A, C) or dexamethasone (B, D). (E-F) Box plots of neurite length per neuromast (E) and neurite length per hair cell (F), with whiskers at min/max and mean values marked with "+". Data for each experimental trial were normalized to the median value of unlesioned controls. Regenerating neuromasts (orange plots) in dexamethasone-treated fish had significantly longer neurites per neuromast (E) (****adjusted P<0.0001), however the difference in length in dexamethasone-treated fish was not significant relative to the total number of hair cells/neuromast, when compared to DMSO controls (F). N=4-7 fish per condition per trial; 6 experimental trials.

processes per neuromast was significantly greater in animals that recovered in dexamethasone compared to animals exposed to drug carrier alone (Fig 3 C-E (orange box plots); ****adjusted P<0.0001; Tukey's multiple comparisons test). We reasoned that increased neurite length in dexamethasone-treated animals was related to the greater number of regenerated hair cells per neuromast. To verify this idea, neurite length was normalized relative to the number of hair cells in each neuromast. Following normalization, we observed no difference in relative neurite length

305 per hair cell in animals recovered in dexamethasone vs. those in drug carrier alone (Fig 3F
306 (orange box plots); adjusted P=0.5630). In unlesioned animals treated with dexamethasone, we
307 observed no change in afferent neurite length per neuromast (Fig. 3 A,B,E (gray box plots);
308 adjusted P=0.8215) and a modest reduction in the relative neurite length per hair cell that was
309 not statistically significant (Fig 3F (gray box plots); adjusted P=0.2959). These data indicate that
310 dexamethasone treatment enhanced the formation of afferent processes in regenerating
311 neuromasts, perhaps to accommodate a greater number of regenerated hair cells. By contrast,
312 in unlesioned neuromasts dexamethasone did not promote the addition of afferent neurites to
313 accommodate additional hair cells.

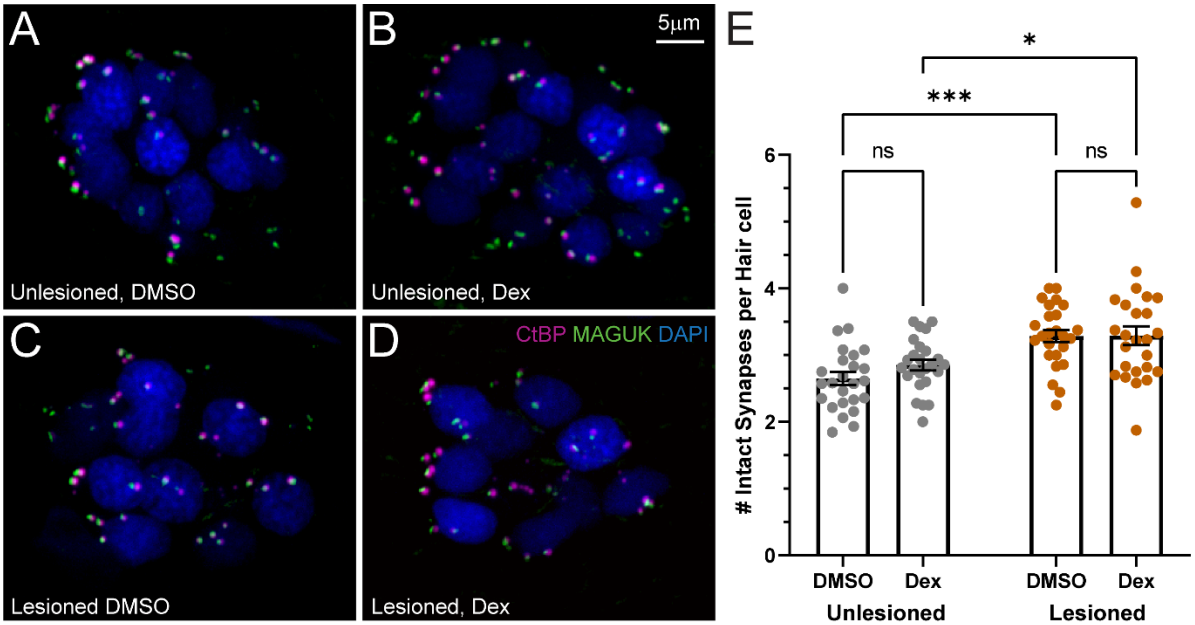

Figure 4. Dexamethasone exposure did not alter the number of afferent synapses in neuromast hair cells (A-D) Representative maximum intensity projection images of 7dpf pLL neuromasts, with hair cell presynaptic ribbons labeled via CtBP antibody (magenta), post-synaptic densities labeled via MAGUK antibody (green), and hair cell nuclei labeled with DAPI (blue). Neuromasts were either unlesioned (A, B) or lesioned with $CuSO_4$ (C, D), then allowed to regenerate for 48 hr while exposed to DMSO (carrier) (A, C) or dexamethasone (B, D). (E) Scatter plots with mean and SEM bars showing no significant difference in the number of intact synapses in dexamethasone-treated fish, compared to DMSO controls for both lesioned and intact neuromasts. Each dot represents a single neuromast on an individual fish.Notably, a significantly greater number of intact synapses per hair cell were observed in regenerating neuromasts relative to neuromasts that were not lesioned (adjusted ***P=0.0003 (DMSO), * P=0.0202 (Dex)). N=5 fish per condition per trial; 4 experimental trials.

314 In addition to quantifying hair cell numbers and neurite length, we also quantified the
315 number of intact synapses per hair cell (Fig. 4 A-D; defined as presynaptic ribbons adjacent to
316 postsynaptic densities). We observed no difference in synapse counts between
317 dexamethasone-treated and 0.1% DMSO controls when comparing unlesioned neuromasts or
318 when comparing $CuSO_4$ lesioned neuromasts following regeneration (Fig. 4 E). Notably, we did
319 observe significantly more intact synapses per hair cell in all regenerating neuromasts relative to

unlesioned neuromasts (Fig 4 E; adjusted ***P=0.0003 (DMSO), * P=0.0202 (Dex); Tukey's multiple comparisons test). Similar observations have been reported in regenerating neuromast hair cells (Hardy et al., 2021; Suli et al., 2016) and may reflect ongoing synaptic refinement akin to that observed in developing cochlear hair cells (Michanski et al., 2019). Overall, these results suggest that dexamethasone treatment enhances afferent neurite outgrowth in regenerating neuromasts and does not impact synapse formation in newly formed hair cells in regenerating or unlesioned neuromasts.

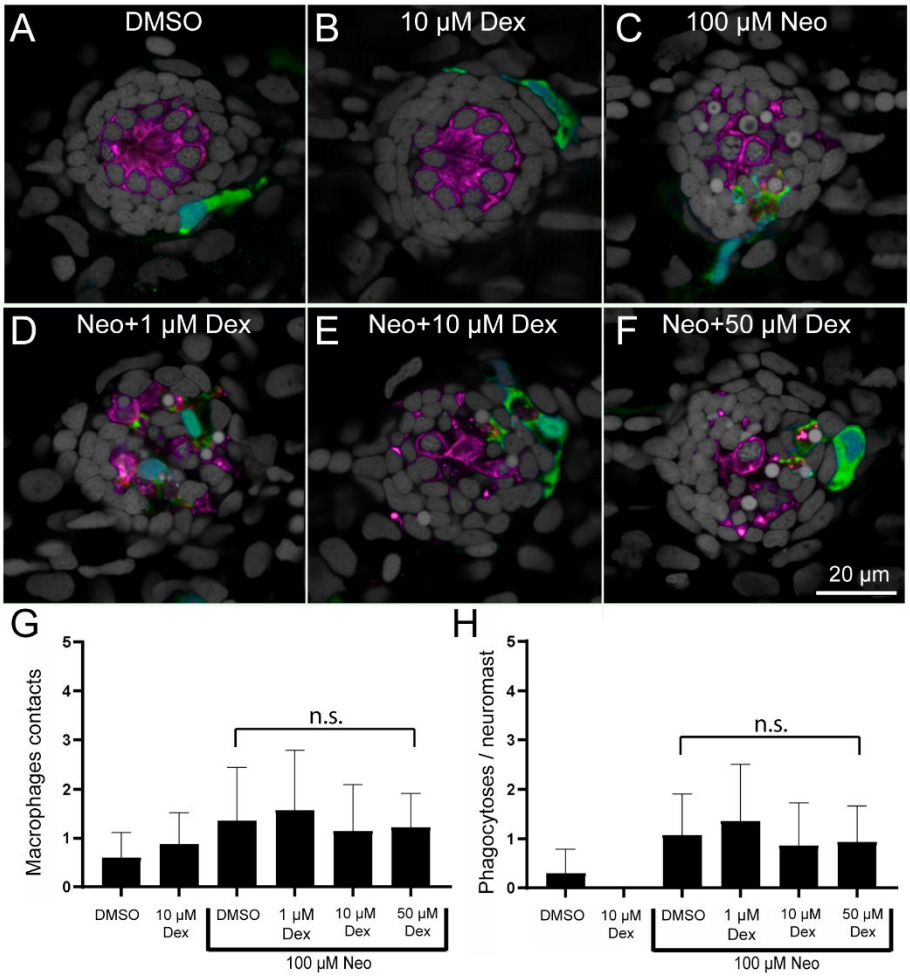

Figure 5. Dexamethasone did not inhibit macrophage response to neuromast injury

(A-F) Representative confocal images of control (A,B) and neomycin injured neuromasts (C-F). Larvae (6 dpf) were treated for 24 h with dexamethasone, then exposed for 30 min to neomycin. All specimens were fixed and processed for labeling of macrophages (green, YFP), hair cells (magenta, Otoferlin) and nuclei (gray, DAPI). Normal localization of macrophages was observed in control fish (A,B) and no inhibition was observed in neuromasts treated with neomycin (C-F). (G-H) Dexamethasone pretreatment did not affect macrophage contacts with dying hair cells (G, P>0.9999, Dunn's multiple comparison test) or the number of phagocytotic events (H, P>0.9999, Dunn's multiple comparison test). Bars indicate SD. N=15 fish/group; 2 experimental trials.

Pretreatment with dexamethasone does not inhibit macrophage response to hair cell injury

Dexamethasone inhibits inflammation and macrophage activation, and various studies indicate dexamethasone's anti-inflammatory action can influence nerve regeneration (Valledor & Ricote, 2004). Previous work has shown that macrophages are recruited to lateral-line organs after injury induced by the ototoxin neomycin (Warchol et al., 2021). We therefore assessed whether dexamethasone inhibited macrophage entry and phagocytosis after application of the

ototoxin neomycin. We quantified macrophage entry and phagocytosis in response to neomycin treatment after pretreating larvae for 24 hr with 1, 10 or 50 μM dexamethasone. Larvae that were not exposed to either neomycin and/or dexamethasone served as controls (Fig 5 A). All experiments followed the same protocol that we had previously used to characterize macrophage recruitment and phagocytosis after neomycin toxicity (Warchol et al., 2021). Dexamethasone treatment did not induce any significant changes to macrophage contacts in the absence of neomycin (Fig 5 B) or to the subsequent macrophage response following neomycin lesion (Fig. 5 C-F*)*. Quantification revealed that the number of macrophage-hair cell contacts (Fig. 5 G) and number of phagocytotic events (Fig. 5 H) was similar in all neomycin treatment groups. These observations indicate that pre- and co-treatment with 10 μM dexamethasone does not suppress macrophage activation in response to neuromast injury.

Hair cell FM1-43 uptake and calcium homeostasis is unaffected by dexamethasone exposure

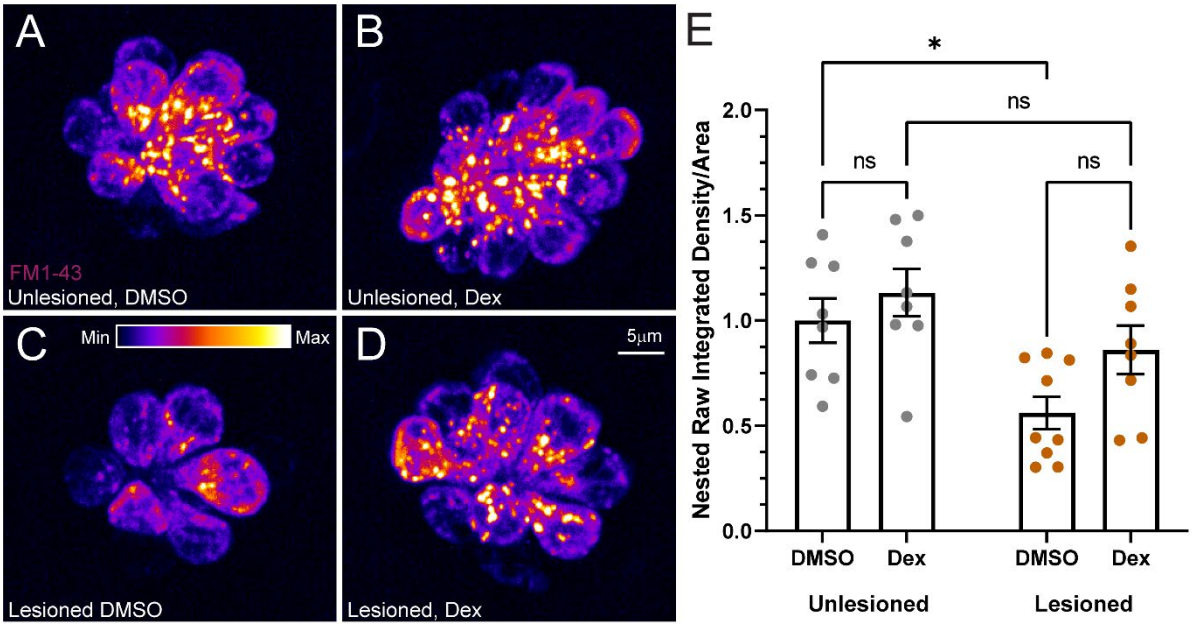

Figure 6. FM1-43 uptake was not significantly affected by dexamethasone exposure

(A-D) Representative maximum intensity projection images of pLL neuromasts in live 7dpf larvae immediately after brief (20 seconds) FM1-43 exposure. Neuromasts were either left intact (A, B) or lesioned with $CuSO_4$ (C, D), then allowed to regenerate for 48 hr while exposed to DMSO (carrier) (A, C) or dexamethasone (B, D) prior to FM1-43 exposure. The LUT bar (C) shows the range of intensity values, starting at 0 (min) to 400 (max). (E) Relative average FM1-43 intensity per neuromast. Scatter plots show raw integrated density (i.e. sum of the pixel values)/area values with SEM bars. Each dot represents the average values of neuromasts L3-L5 for one fish. Values were normalized for each experiment using the inverse median of the unlesioned control values. The data show no significant differences in intensity for dexamethasone-treated fish, relative to DMSO controls, in both intact and regenerating neuromasts (adjusted *P=0.0226). N=2-3 fish per condition per trial; 4 experimental trials.

Numerous studies have indicated that dexamethasone can induce mitochondrial dysfunction in various tissues, including adipocytes (Luan et al., 2019), skeletal muscle (Liu et al., 2016), and neurons (Du et al., 2009). We previously reported reduced hair cell uptake of the cationic dye FM1-43 in zebrafish mutants with impaired hair cell mitochondrial function (*mpv17*$^{-/-}$), indicating that these fish possessed reduced driving force for cations through mechanotransduction channels, and elevated hair cell mitochondrial calcium (Holmgren & Sheets, 2021). We therefore evaluated whether 48-hour dexamethasone exposure affected hair cell uptake of FM1-43 and calcium homeostasis. We

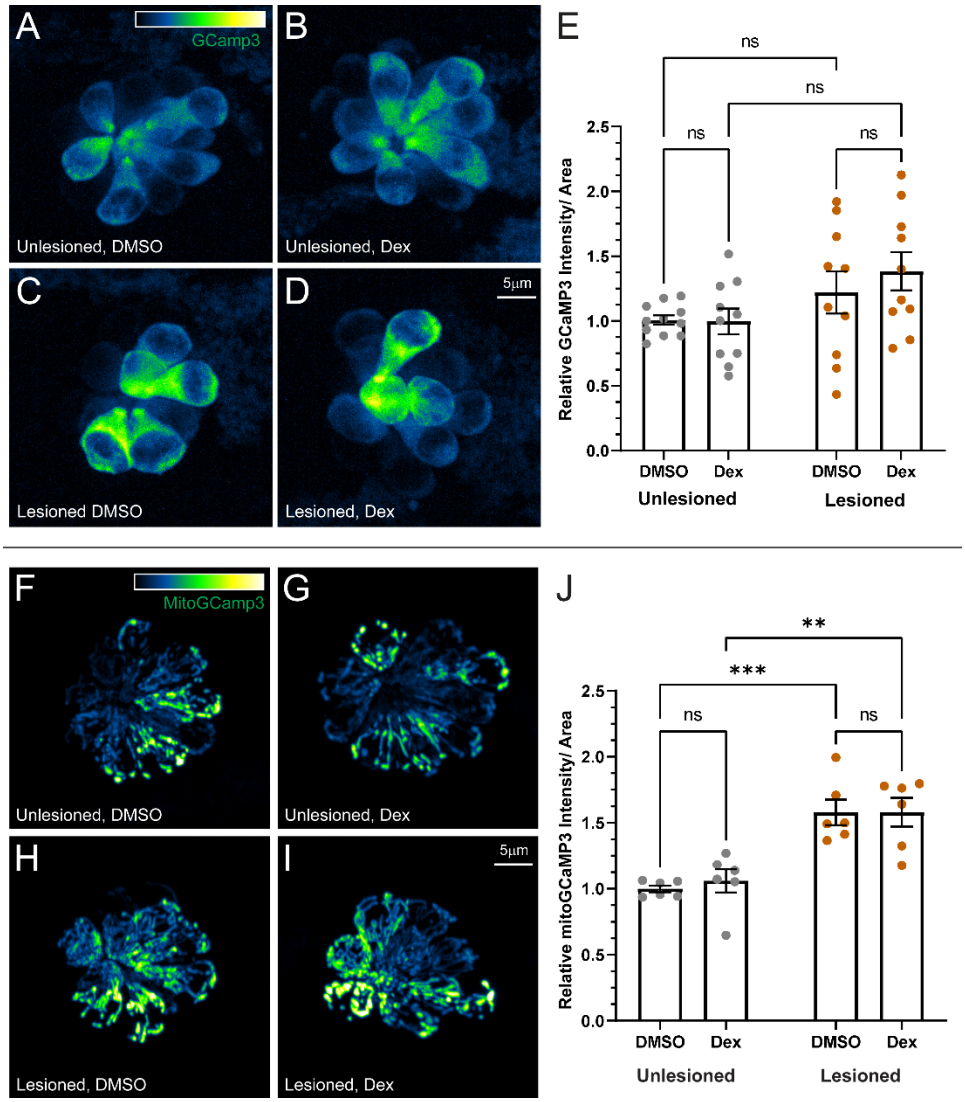

Figure 7. Dexamethasone did not affect hair cell cytosolic or mitochondrial calcium homeostasis

(A-D) Representative maximum intensity projection images of neuromasts in live 7dpf Tg(-6myo6b: GCaMP3) larvae. The LUT bar in (A) shows range of intensity values starting at 0 (min) to 2150 (max). (E) Hair cell GCaMP3 fluorescence intensity is not affected by dexamethasone exposure. Scatter plots of relative raw integrated intensity/area values with SEM bars. Each dot represents the average values of neuromasts L3-L5 for one fish. Data show no significant differences in intensity for dexamethasone-treated fish relative to DMSO controls in both intact and regenerating neuromasts. N=2-3 fish per condition per trial; 5 experimental trials (F-I) Representative images neuromasts in Tg(-6myo6b: mitoGCaMP3) larvae. LUT bar (F) shows range of intensity values starting at 0 (min) to 300 (max). (J) Hair cell mitoGCaMP fluorescence intensity is not affected by dexamethasone exposure but is elevated in regenerating neuromasts relative to intact neuromasts. Data show no significant differences in intensity for dexamethasone-treated fish relative to DMSO controls in both intact and regenerating neuromasts (adjusted ***P=0.0006 (DMSO), **P=0.0019 (Dex)). N=2-3 fish per condition per trial; 3 experimental trials.

observed no differences in FM1-43 uptake in unlesioned neuromasts that were treated in dexamethasone vs. those incubated in DMSO carrier (Fig. 6 A,B,E (gray circles)). In regenerating neuromasts, dexamethasone treatment appeared to cause a modest increase in FM1-43 uptake, but this trend did not reach statistical significance (Fig. 6 C-E (orange circles); adjusted P=0.1786; Tukey's multiple comparisons test). Notably, hair cells in regenerating DMSO-treated neuromasts (Fig. 6 C) displayed significantly reduced FM1-43 uptake relative to unlesioned DMSO-treated neuromasts (Fig. 6 A,E; adjusted *P=0.0226), indicating reduced mechanotransduction in regenerated control neuromast hair cells. By contrast, there was no significant difference in FM1-43 uptake in regenerating vs. unlesioned dexamethasone-treated neuromast hair cells (Fig. 6 B,D,E; adjusted P=0.2747), suggesting that dexamethasone treatment during regeneration may enhance hair cell regeneration and may also slightly impact the maturation of mechanotransduction.

We next examined hair cell cytosolic and mitochondrial calcium homeostasis using the genetically encoded calcium indicator GCaMP3 (Esterberg et al., 2013; Esterberg et al., 2014). When comparing unlesioned neuromasts and $CuSO_4$ lesioned neuromasts following regeneration, we observed average cytosolic calcium levels did not differ in neuromast hair cells (Fig. 7 A-E), while mitochondrial calcium levels appeared significantly higher in regenerating neuromast hair cells relative to unlesioned in both DMSO and dexamethasone treatment conditions (Fig. 7 F-J; adjusted ***P=0.0006 (DMSO), **P=0.0019 (Dex); Tukey's multiple comparisons test). Notably, dexamethasone treatment had no effect on cytosolic or mitochondrial calcium levels relative to DMSO control in both unlesioned and regenerating neuromasts (Fig. 7 E, J). Cumulatively, these data suggest that prolonged dexamethasone exposure does not significantly impact hair cell mechanotransduction or affect calcium homeostasis in either intact or regenerating neuromasts.

Prolonged dexamethasone exposure hyperpolarizes neuromast mitochondria and sensitizes hair cells to neomycin

To determine whether 48-hour dexamethasone exposure impacted mitochondrial function in lateral-line neuromasts, we examined mitochondrial membrane potentials ($\Delta\Psi m$) in unlesioned neuromast hair cells and supporting cells using tetramethylrhodamine methyl ester (TMRE)—a cell-permeant cationic dye used to assess mitochondrial function (Alassaf et al., 2019; Esterberg et al., 2016). Dexamethasone-exposed neuromasts had significantly higher TMRE mean fluorescence intensity relative to controls (Fig. 8 A,B,E; **** P<0.0001; Welch's t-test), indicating that mitochondria in dexamethasone-exposed neuromast cells are more hyperpolarized. Elevated TMRE fluorescence was apparent not only in the mitochondria of hair

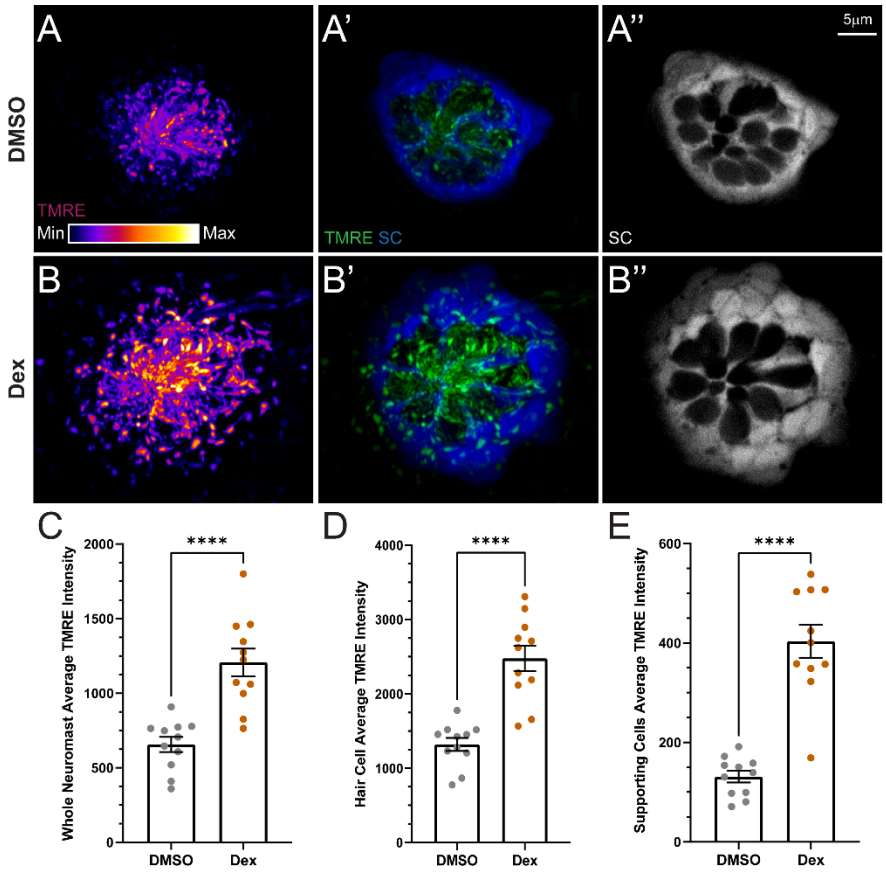

Figure 8. Dexamethasone exposure elevated mitochondrial activity in hair cells and supporting cells
(A-B) Confocal images of neuromasts in 7dpf fish following TMRE exposure. Fish were treated with DMSO (A) or dexamethasone (B) for 48 hours prior to imaging. TMRE (A, A', B, B') is shown as a max intensity projection and supporting cell (SC) images (A', A'', B', B'') are z-slices from the midlevel of the neuromast. Negative spaces inside GFP-labeled supporting cells indicate neuromast hair cells. LUT bar (A) shows range of intensity values starting at 0 (min) to 11800 (max). (E-G) Scatter plots of average TMRE fluorescence intensity with SEM bars. Dexamethasone-treated fish had significantly hyperpolarized mitochondria in both neuromast hair cells and supporting cells (adjusted **** P<0.0001). N=1-4 fish per condition per trial; 5 experimental trials.

cells (Fig 8 A', B', F; EGFP-negative cells), but also the surrounding supporting cells (Fig 8 A", B", G; EGFP-positive cells), suggesting prolonged dexamethasone exposure disrupts normal mitochondrial function in both hair cells and supporting cells. Given that the hair cells in dexamethasone-treated larvae had more negatively charged ΔΨm, we predicted that these hair cells would be more vulnerable to neomycin-induced hair cell death (Alassaf et al., 2019; Holmgren & Sheets, 2021). We therefore compared neomycin-induced hair cell lesion in fish pre-treated with dexamethasone or DMSO carrier alone (Fig 9 A-J). When treated with higher doses of neomycin (50-100 µM), we observed significantly more lateral-line hair cell loss in fish pre-exposed for 48 hours to dexamethasone, relative to controls (Fig 9 K; adjusted P= 0.1407 (30 µM), *P=0.0353 (50 µM), ****P<0.0001 (100 µM); Šídák's multiple comparisons test). Thus, while prolonged dexamethasone does not appear to impact cytosolic or mitochondrial calcium homeostasis, it does alter neuromast mitochondrial function and increases hair cell sensitivity to neomycin-induced death.

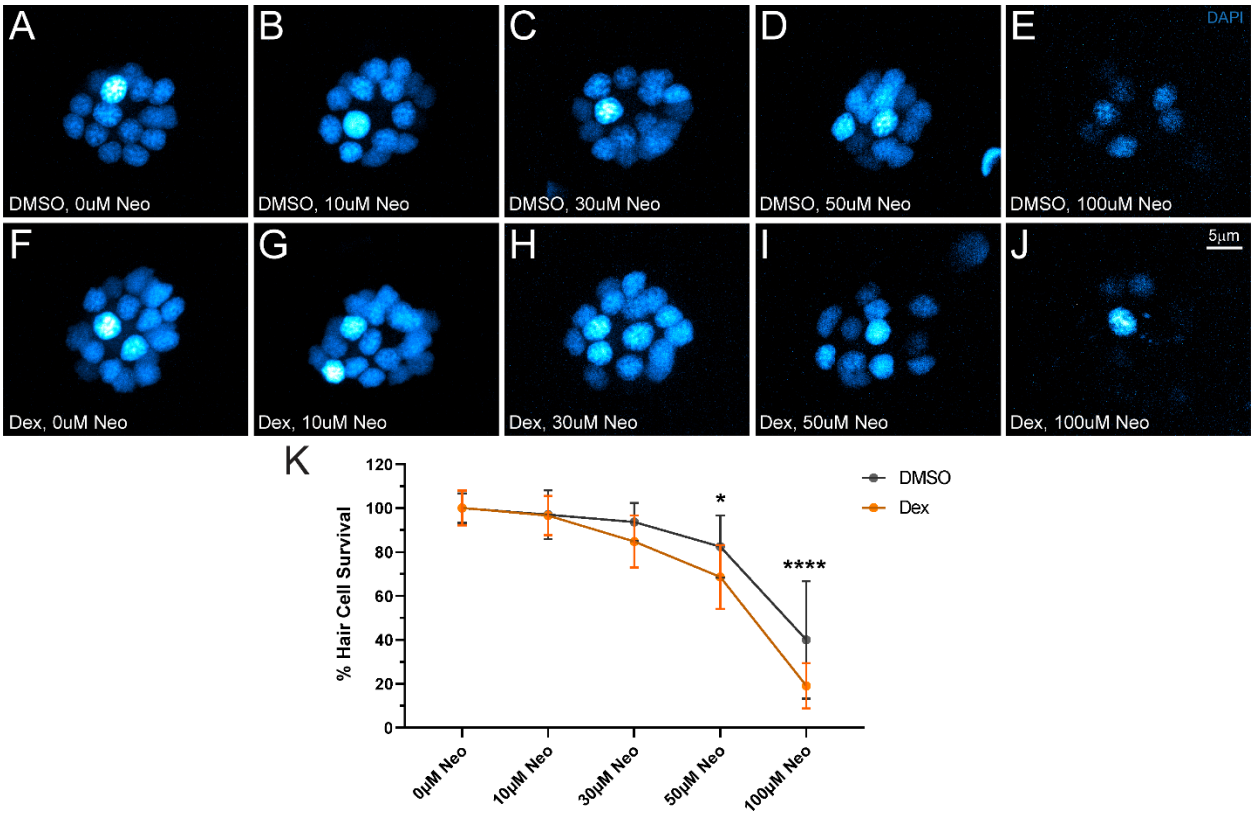

Figure 9. Dexamethasone exposure increased hair cell sensitivity to neomycin

(A-J) Representative maximum intensity images of DAPI-labeled neuromast hair cell nuclei (blue). Larvae (7dpf) were exposed for 48 hr to DMSO (carrier) alone (A-E) or dexamethasone (F-J), then exposed for 30min or 10µM (B, G), 30µM (C, H), 50µM (D, I), or 100µM (E, J) neomycin. EM buffer alone was used as a control (A,F). (K) Dose response curve with mean and SEM bars shows the number of surviving hair cells per neuromast as a percent of those present in unlesioned controls. Dexamethasone-treated neuromast hair cells were more sensitive to neomycin induced cell death than controls (adjusted P= 0.1407 (30 µM), *P=0.0353 (50 µM), ****P<0.0001 (100 µM)). N=7 fish per condition per trial; 3 experimental trials.

Prolonged dexamethasone exposure reduces evoked calcium influx through mechanosensory hair bundles

Hair cells respond to sensory stimuli via deflection of apical hair bundles and opening of mechanotransduction channels. Influx of potassium and calcium occurs through these channels which depolarizes the hair cell, leading to influx of calcium through basally-localized presynaptic voltage-gated calcium channels, and triggering release of synaptic vesicles (Corey & Hudspeth, 1979; Moser & Beutner, 2000; Zhang et al., 2018). To determine if prolonged dexamethasone exposure influenced hair cell responses to mechanical stimulation, we measured evoked calcium influx at hair bundles and hair cell synapses in response to bundle deflection using a transgenic line expressing plasma-membrane targeted GCaMP6s (Fig. 10 A ;(Sheets et al., 2017)). In response to a 500 ms step deflection, calcium influx at the hair bundle was significantly reduced in dexamethasone-treated larvae relative to controls (Fig 10 B, B';

441 **P=0.0052; Unpaired t-test); an unexpected result given that uptake of the cationic dye FM1-43
442 was not reduced in dexamethasone-treated larvae (Fig. 5 A, B, E). By contrast, presynaptic
443 calcium influx was not significantly different in dexamethasone-treated fish vs. controls (Fig. 10
444 C, D). Baseline GCaMP6sCAAX measurements at neuromast hair bundles and hair cell
445 presynaptic regions were comparable between dexamethasone-treated and control animals
446 (Fig. 10 E, F), indicating that calcium levels at rest were not altered in these two subcellular
447 compartments. Overall, these results provide evidence that prolonged dexamethasone
448 exposure does not affect hair cell calcium homeostasis but does negatively influence calcium
449 flow through the hair bundle in response to stimulus.

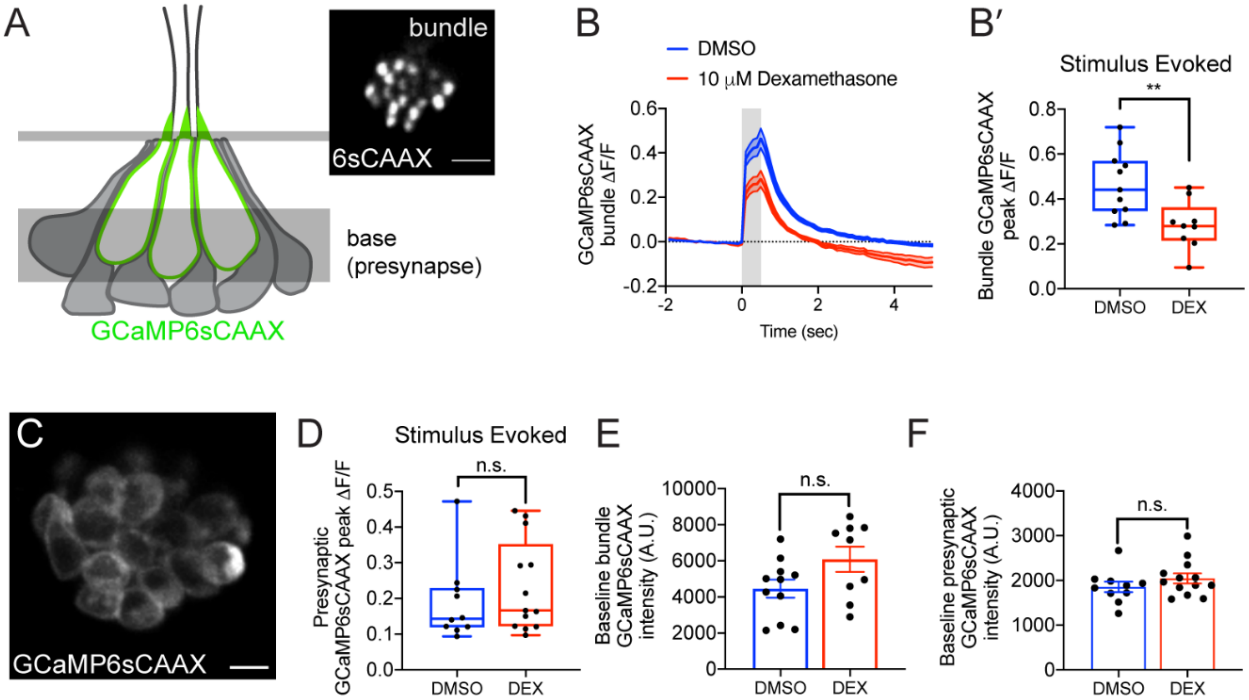

Figure 10. Dexamethasone exposure decreased evoked mechanosensation but not presynaptic calcium responses

(A) Schematic of a neuromast viewed from the side, and the imaging planes used to measure evoked calcium activity at the hair bundles and at the presynaptic region. Localization of GCaMP6sCAAX is shown in green. Inset shows an example of a top-down view of the hair bundle plane showing GCaMP6sCAAX fluorescence. (B-B') Evoked hair bundle calcium signal with (red) or without (blue) 48-hour dexamethasone pretreatment. Average traces are shown in B, while dot plots of peak response of bundles per neuromast are shown in B'. (C) Top-down view of the basal plane showing the presynaptic membrane labeled with GCaMP6sCAAX. (D) Dot plots show that the peak evoked presynaptic calcium signal averaged per neuromast with (red) and without (blue) 48-hour dexamethasone pretreatment. (E-F) Baseline calcium intensity with (red) and without (blue) dexamethasone treatment in hair bundles (E) and presynapses (F) Shaded area above and below traces in panel B and error bars in E-F represent SEM. Box-and-whiskers plot were used in B' and D to show median, min and max. An unpaired Welch's unequal variance *t*-test was used to calculate the significance of differences in B' and D. An unpaired *t*-test was used to calculate the significance of differences in E-F. n ≥ 9 neuromasts per treatment. **P=0.0052. Scale bar = 5 μm in A inset and C.

450 Discussion

451 Dexamethasone is a potent synthetic glucocorticoid that influences diverse molecular
452 pathways involved in cellular development, homeostasis, and repair. Using the zebrafish lateral
453 line as a model for hair cell organs, we examined the influence of prolonged dexamethasone
454 exposure on both afferent innervation of newly generated hair cells as well as hair cell
455 homeostasis and function. Following 48 hours of dexamethasone exposure, we observed no
456 inhibition of innervation or synapse formation in newly generated neuromast hair cells, indicating
457 that dexamethasone did not inhibit regeneration of afferent synaptic contacts in the lateral-line
458 system. However, further examination revealed prolonged dexamethasone exposure induced
459 mitochondrial hyperpolarization in neuromast hair cells and supporting cells, suggesting
460 disruption of mitochondrial homeostasis. In addition, dexamethasone exposure specifically
461 reduced evoked calcium influx at the hair bundle but not the hair cell synapse in response to
462 water-jet stimulus. Cumulatively, our data support that prolonged dexamethasone does not
463 inhibit newly generated hair cell innervation or synapse formation, but it may negatively impact
464 hair cell energy homeostasis and function.

465 **Dexamethasone did not inhibit lateral-line afferent nerve regrowth or hair cell synapse**
466 **formation during regeneration**

467 Exposure to dexamethasone significantly increased the total length of afferent neurites
468 per regenerating neuromast (Fig 3 C-E). The addition in nerve fiber length corresponds to the
469 increased number of hair cells (Fig. 3 F), suggesting that nerve fiber length was increased in
470 regenerating neuromasts to accommodate a larger number of newly formed hair cells.
471 Alternatively, it is possible that the additional neurites may be involved in facilitating hair cell
472 generation. A recent study characterizing functional lateral-line neuromast regeneration
473 following $CuSO_4$ ablation has reported that afferent nerve terminals formed initial contacts with
474 supporting cells during regeneration, suggesting that afferent nerve contacts may help facilitate
475 transdifferentiation of supporting cells into hair cells (Hardy et al., 2021). However, while
476 dexamethasone treatment caused regenerating neuromasts to add additional afferent dendrite
477 length, no such increase was observed in unlesioned neuromasts (Fig. 3 A,B,E), suggesting
478 that the generation of additional hair cells in unlesioned neuromasts is not facilitated by
479 additional nerve fiber contacts. Given that dexamethasone treatment did not increase the
480 number of afferent synapses per hair cell in unlesioned neuromasts (Fig 4 E; gray circles), we
481 posit that afferent neurons innervate and form synapses with newly generated hair cells in
482 unlesioned larval neuromasts without adding additional processes.

483 We also did not observe inhibition of macrophage activation in response to ototoxic
484 damage following dexamethasone pretreatment (Fig 5). This result provides additional support
485 to a previously reported observation that dexamethasone likely enhances neuromast
486 regeneration via a mechanism other than immunosuppression (Namdaran et al., 2012). Instead,
487 dexamethasone may be acting though glucocorticoid receptors to enhance division of a subset
488 of hair cell precursors. Further studies will be needed explore the cellular pathways underlying
489 dexamethasone-induced hair cell generation, and the mechanistic differences between afferent
490 nerve innervation and synapse formation in regenerating vs. intact neuromasts.

491 **Prolonged dexamethasone exposure modulates mitochondrial membrane potential in**
492 **neuromast cells and enhances neomycin hair cell toxicity**

493 Glucocorticoid receptors reside in the cytosol of cells. When activated by a ligand such
494 as cortisol or dexamethasone, they regulate gene expression by localizing to the cell nucleus
495 and either directly binding to DNA or altering the activity of transcription factors or various
496 kinases (Oakley & Cidlowski, 2013). Activated glucocorticoid receptors have also been shown to
497 translocate into the mitochondria and regulate mitochondrial gene expression (Kokkinopoulou &
498 Moutsatsou, 2021), and previous studies of mouse liver and rat distal colon have reported
499 enhanced expression of mitochondrial genes involved in oxidative phosphorylation following
500 dexamethasone treatment (Li et al., 2016; Rachamim et al., 1995). The glucocorticoid receptor
501 gene *nr3c1* has been shown to be expressed in larval zebrafish neuromast hair cells and all
502 populations of supporting cells (Lush et al., 2019). Speculatively, prolonged dexamethasone
503 exposure may be modulating the expression of mitochondrial DNA encoded genes involved in
504 oxidative phosphorylation, thereby altering mitochondrial metabolism in neuromast hair cells
505 and supporting cells.

506 A recent study assessing the effects of cortisol exposure on hair cell sensitivity to
507 neomycin further supports the hypothesis that activated glucocorticoid receptors regulates
508 expression of genes that modulate mitochondrial metabolism (Hayward et al., 2019). Those
509 authors reported that pretreatment of zebrafish larvae with cortisol for 24 hours sensitized
510 neuromast hair cells to neomycin-induced hair cell death, which is comparable to what we
511 observed in dexamethasone-treated fish (Fig. 9). Cortisol-mediated sensitization to neomycin
512 was dependent on glucocorticoid receptor activation and could be blocked by inhibiting protein
513 translation. It is worth noting that Hayward et al. did not report a similar sensitization to
514 neomycin following 24 h dexamethasone exposure, but it is likely dexamethasone and cortisol
515 are acting through a shared mechanism. The difference between their reported observations
516 and our results is probably due to two factors. First, the concentration of neomycin used in

517 Hayward et al. following dexamethasone was 25 μM, which was two-fold less than the dose at
518 which we first observed significant effects ((Hayward et al., 2019); Fig 9 K). Also, the
519 dexamethasone pretreatment doses (0.001-1 μM vs. 10 μM) and exposure time (24 vs. 48
520 hours) used by Haywood et al., (2019) were less than those used in the present study.

521 **Prolonged dexamethasone exposure reduces evoked calcium influx though**
522 **mechanotransduction channels but does not affect hair cell calcium homeostasis**

523 While we did observe hyperpolarization of mitochondrial membrane potential in
524 dexamethasone-exposed neuromasts (Fig. 8), we did not observe significant changes in
525 cytosolic or mitochondrial calcium homeostasis within hair cells relative to controls (Fig 7). By
526 contrast, in response to water-jet stimuli, evoked calcium influx at the hair bundle was
527 significantly reduced (Fig. 10 B), suggesting calcium influx through activated MET channels is
528 reduced. This observed effect on calcium influx specifically at the hair bundle may be a
529 consequence of altered mitochondrial metabolism. Mitochondria are important regulators of
530 local intracellular calcium levels in sensory hair cells, and in addition to directly taking up
531 calcium, mitochondria provide ATP to drive clearance of calcium though plasma membrane
532 Ca^{2+}-ATPases (PMCA1 and PMCA2), with PMCA2 shown to be densely localized in the hair cell
533 stereocilia (Beurg et al., 2010). Zebrafish homologues of PMCA1 and PMCA2 are strongly
534 expressed in mature neuromast hair cells of larval zebrafish (Lush et al., 2019). It is possible
535 that altered mitochondrial metabolism may be influencing the activity of PMCA2 in
536 dexamethasone-treated hair cells, thereby modifying PMCA2 regulation of calcium levels at the
537 hair bundle. It is also conceivable that activated glucocorticoid receptors may be modulating
538 expression of genes involved in mechanotransduction channel calcium permeability. Further
539 experiments will be needed to determine the mechanism underlying dexamethasone's specific
540 effect on calcium influx through stimulated hair bundles.

541 In conclusion, our observations from zebrafish lateral-line neuromasts indicate that 48-
542 hour dexamethasone treatment enhances regeneration and afferent reinnervation but alters
543 mitochondrial homeostasis and evoked calcium influx through hair bundles. Dexamethasone is
544 a steroid commonly used for treating hearing loss, and identifying strategies to retain high levels
545 of dexamethasone for long periods within the inner ear is currently an active area of research.
546 Considering our observations showing that prolonged exposure to dexamethasone had an
547 adverse effect on hair cell mitochondrial metabolism and impacted hair bundle calcium influx,
548 we believe future studies on the effects of long-term, localized dexamethasone treatment on
549 mammalian cochlear function are indicated.

Declaration of interests: The authors declare no competing financial or non-financial interests.

Acknowledgments: This work was supported by the RNID (Project ID G85; L.S.), a National Institute on Deafness and Other Communication Disorders (NIDCD) Intramural Research Program Grant 1ZIADC000085-01 (K.S.K), and Extramural Research Project Grant R01DC006283 (M.E.W.).

References

Alassaf, M., Daykin, E. C., Mathiaparanam, J., & Wolman, M. A. (2019). Pregnancy-associated plasma protein-aa supports hair cell survival by regulating mitochondrial function. *Elife*, *8*. https://doi.org/10.7554/eLife.47061

Behra, M., Gallardo, V. E., Bradsher, J., Torrado, A., Elkahloun, A., Idol, J., Sheehy, J., Zonies, S., Xu, L., Shaw, K. M., Satou, C., Higashijima, S., Weinstein, B. M., & Burgess, S. M. (2012). Transcriptional signature of accessory cells in the lateral line, using the Tnk1bp1:EGFP transgenic zebrafish line. *BMC Dev Biol*, *12*, 6. https://doi.org/10.1186/1471-213X-12-6

Beurg, M., Nam, J. H., Chen, Q., & Fettiplace, R. (2010). Calcium balance and mechanotransduction in rat cochlear hair cells. *J Neurophysiol*, *104*(1), 18-34. https://doi.org/10.1152/jn.00019.2010

Bremer, J., Skinner, J., & Granato, M. (2017). A small molecule screen identifies in vivo modulators of peripheral nerve regeneration in zebrafish. *PLoS One*, *12*(6), e0178854. https://doi.org/10.1371/journal.pone.0178854

Coffin, A. B., Rubel, E. W., & Raible, D. W. (2013). Bax, Bcl2, and p53 differentially regulate neomycin- and gentamicin-induced hair cell death in the zebrafish lateral line [Research Support, N.I.H., Extramural

Research Support, Non-U.S. Gov't]. *Journal of the Association for Research in Otolaryngology : JARO*, *14*(5), 645-659. https://doi.org/10.1007/s10162-013-0404-1

Corey, D. P., & Hudspeth, A. J. (1979). Ionic basis of the receptor potential in a vertebrate hair cell. *Nature*, *281*(5733), 675-677. https://doi.org/10.1038/281675a0

Du, J., Wang, Y., Hunter, R., Wei, Y., Blumenthal, R., Falke, C., Khairova, R., Zhou, R., Yuan, P., Machado-Vieira, R., McEwen, B. S., & Manji, H. K. (2009). Dynamic regulation of mitochondrial function by glucocorticoids. *Proc Natl Acad Sci U S A*, *106*(9), 3543-3548. https://doi.org/10.1073/pnas.0812671106

Egli Gallo, D., Khojasteh, E., Gloor, M., & Hegemann, S. C. (2013). Effectiveness of systemic high-dose dexamethasone therapy for idiopathic sudden sensorineural hearing loss. *Audiol Neurootol*, *18*(3), 161-170. https://doi.org/10.1159/000346938

Esterberg, R., Hailey, D. W., Coffin, A. B., Raible, D. W., & Rubel, E. W. (2013). Disruption of intracellular calcium regulation is integral to aminoglycoside-induced hair cell death [Research Support, N.I.H., Extramural]. *The Journal of neuroscience : the official journal of the Society for Neuroscience*, *33*(17), 7513-7525. https://doi.org/10.1523/JNEUROSCI.4559-12.2013

Esterberg, R., Hailey, D. W., Rubel, E. W., & Raible, D. W. (2014). ER-mitochondrial calcium flow underlies vulnerability of mechanosensory hair cells to damage [Research Support, N.I.H., Extramural]. *The Journal of neuroscience : the official journal of the Society for Neuroscience*, *34*(29), 9703-9719. https://doi.org/10.1523/JNEUROSCI.0281-14.2014

Esterberg, R., Linbo, T., Pickett, S. B., Wu, P., Ou, H. C., Rubel, E. W., & Raible, D. W. (2016). Mitochondrial calcium uptake underlies ROS generation during aminoglycoside-induced hair cell death. *J Clin Invest*, *126*(9), 3556-3566. https://doi.org/10.1172/JCI84939

596 Feng, X., & Yuan, W. (2015). Dexamethasone enhanced functional recovery after sciatic nerve
597 crush injury in rats. *Biomed Res Int*, *2015*, 627923. https://doi.org/10.1155/2015/627923
598 Fernandez, R., Harrop-Jones, A., Wang, X., Dellamary, L., LeBel, C., & Piu, F. (2016). The
599 Sustained-Exposure Dexamethasone Formulation OTO-104 Offers Effective Protection
600 against Cisplatin-Induced Hearing Loss. *Audiol Neurootol*, *21*(1), 22-29.
601 https://doi.org/10.1159/000441833
602 Ge, H., Ni, S., Wang, X., Xu, N., Liu, Y., Wang, X., Wang, L., Song, D., Song, Y., & Bai, C.
603 (2012). Dexamethasone reduces sensitivity to cisplatin by blunting p53-dependent
604 cellular senescence in non-small cell lung cancer. *PLoS One*, *7*(12), e51821.
605 https://doi.org/10.1371/journal.pone.0051821
606 Hardy, K., Amariutei, A. E., De Faveri, F., Hendry, A., Marcotti, W., & Ceriani, F. (2021).
607 Functional development and regeneration of hair cells in the zebrafish lateral line. *J*
608 *Physiol*, *599*(16), 3913-3936. https://doi.org/10.1113/JP281522
609 Hayward, T., Young, A., Jiang, A., Crespi, E. J., & Coffin, A. B. (2019). Glucococorticoid
610 receptor activation exacerbates aminoglycoside-induced damage to the zebrafish lateral
611 line. *Hear Res*, *377*, 12-23. https://doi.org/10.1016/j.heares.2019.03.002
612 Holmgren, M., & Sheets, L. (2021). Influence of Mpv17 on Hair-Cell Mitochondrial Homeostasis,
613 Synapse Integrity, and Vulnerability to Damage in the Zebrafish Lateral Line. *Front Cell*
614 *Neurosci*, *15*, 693375. https://doi.org/10.3389/fncel.2021.693375
615 Kokkinopoulou, I., & Moutsatsou, P. (2021). Mitochondrial Glucocorticoid Receptors and Their
616 Actions. *Int J Mol Sci*, *22*(11). https://doi.org/10.3390/ijms22116054
617 Li, R., Jia, Y., Pan, S., Li, X., Song, H., & Zhao, R. (2016). Glucocorticoid Receptor Mediates the
618 Effect of High-Fat Diet on Mitochondrial Oxidative Phosphorylation in Mouse Liver. *DNA*
619 *Cell Biol*, *35*(2), 51-58. https://doi.org/10.1089/dna.2015.2932
620 Liao, A. H., Shih, C. P., Li, M. W., Lin, Y. C., Chuang, H. C., & Wang, C. H. (2021).
621 Development of thermosensitive poloxamer 407-based microbubble gel with ultrasound
622 mediation for inner ear drug delivery. *Drug Deliv*, *28*(1), 1256-1271.
623 https://doi.org/10.1080/10717544.2021.1938758
624 Liu, J., Peng, Y., Wang, X., Fan, Y., Qin, C., Shi, L., Tang, Y., Cao, K., Li, H., Long, J., & Liu, J.
625 (2016). Mitochondrial Dysfunction Launches Dexamethasone-Induced Skeletal Muscle
626 Atrophy via AMPK/FOXO3 Signaling. *Mol Pharm*, *13*(1), 73-84.
627 https://doi.org/10.1021/acs.molpharmaceut.5b00516
628 Longair, M. H., Baker, D. A., & Armstrong, J. D. (2011). Simple Neurite Tracer: open source
629 software for reconstruction, visualization and analysis of neuronal processes.
630 *Bioinformatics*, *27*(17), 2453-2454. https://doi.org/10.1093/bioinformatics/btr390
631 Luan, G., Li, G., Ma, X., Jin, Y., Hu, N., Li, J., Wang, Z., & Wang, H. (2019). Dexamethasone-
632 Induced Mitochondrial Dysfunction and Insulin Resistance-Study in 3T3-L1 Adipocytes
633 and Mitochondria Isolated from Mouse Liver. *Molecules*, *24*(10).
634 https://doi.org/10.3390/molecules24101982
635 Lukasz, D., & Kindt, K. S. (2018). In Vivo Calcium Imaging of Lateral-line Hair Cells in Larval
636 Zebrafish. *J Vis Exp*(141). https://doi.org/10.3791/58794
637 Lush, M. E., Diaz, D. C., Koenecke, N., Baek, S., Boldt, H., St Peter, M. K., Gaitan-Escudero,
638 T., Romero-Carvajal, A., Busch-Nentwich, E. M., Perera, A. G., Hall, K. E., Peak, A.,
639 Haug, J. S., & Piotrowski, T. (2019). scRNA-Seq reveals distinct stem cell populations
640 that drive hair cell regeneration after loss of Fgf and Notch signaling. *Elife*, *8*.
641 https://doi.org/10.7554/eLife.44431
642 Mackenzie, S. M., & Raible, D. W. (2012). Proliferative regeneration of zebrafish lateral line hair
643 cells after different ototoxic insults [Research Support, N.I.H., Extramural]. *PLoS One*,
644 *7*(10), e47257. https://doi.org/10.1371/journal.pone.0047257
645 Marshak, T., Steiner, M., Kaminer, M., Levy, L., & Shupak, A. (2014). Prevention of Cisplatin-
646 Induced Hearing Loss by Intratympanic Dexamethasone: A Randomized Controlled

Study. *Otolaryngol Head Neck Surg*, *150*(6), 983-990. https://doi.org/10.1177/0194599814524894

Michanski, S., Smaluch, K., Steyer, A. M., Chakrabarti, R., Setz, C., Oestreicher, D., Fischer, C., Mobius, W., Moser, T., Vogl, C., & Wichmann, C. (2019). Mapping developmental maturation of inner hair cell ribbon synapses in the apical mouse cochlea. *Proc Natl Acad Sci U S A*, *116*(13), 6415-6424. https://doi.org/10.1073/pnas.1812029116

Moser, T., & Beutner, D. (2000). Kinetics of exocytosis and endocytosis at the cochlear inner hair cell afferent synapse of the mouse. *Proc Natl Acad Sci U S A*, *97*(2), 883-888. https://doi.org/10.1073/pnas.97.2.883

Namdaran, P., Reinhart, K. E., Owens, K. N., Raible, D. W., & Rubel, E. W. (2012). Identification of modulators of hair cell regeneration in the zebrafish lateral line [Comparative Study

Research Support, N.I.H., Extramural]. *The Journal of neuroscience : the official journal of the Society for Neuroscience*, *32*(10), 3516-3528. https://doi.org/10.1523/JNEUROSCI.3905-11.2012

Oakley, R. H., & Cidlowski, J. A. (2013). The biology of the glucocorticoid receptor: new signaling mechanisms in health and disease. *J Allergy Clin Immunol*, *132*(5), 1033-1044. https://doi.org/10.1016/j.jaci.2013.09.007

Obholzer, N., Wolfson, S., Trapani, J. G., Mo, W., Nechiporuk, A., Busch-Nentwich, E., Seiler, C., Sidi, S., Sollner, C., Duncan, R. N., Boehland, A., & Nicolson, T. (2008). Vesicular glutamate transporter 3 is required for synaptic transmission in zebrafish hair cells [Research Support, N.I.H., Extramural]. *The Journal of neuroscience : the official journal of the Society for Neuroscience*, *28*(9), 2110-2118. https://doi.org/10.1523/JNEUROSCI.5230-07.2008

Ohnmacht, J., Yang, Y., Maurer, G. W., Barreiro-Iglesias, A., Tsarouchas, T. M., Wehner, D., Sieger, D., Becker, C. G., & Becker, T. (2016). Spinal motor neurons are regenerated after mechanical lesion and genetic ablation in larval zebrafish. *Development*, *143*(9), 1464-1474. https://doi.org/10.1242/dev.129155

Olivari, F. A., Hernandez, P. P., & Allende, M. L. (2008). Acute copper exposure induces oxidative stress and cell death in lateral line hair cells of zebrafish larvae. *Brain Res*, *1244*, 1-12. https://doi.org/10.1016/j.brainres.2008.09.050

Owens, K. N., Coffin, A. B., Hong, L. S., Bennett, K. O., Rubel, E. W., & Raible, D. W. (2009). Response of mechanosensory hair cells of the zebrafish lateral line to aminoglycosides reveals distinct cell death pathways. *Hear Res*, *253*(1-2), 32-41. https://doi.org/10.1016/j.heares.2009.03.001

Patel, M. (2017). Intratympanic corticosteroids in Meniere's disease: A mini-review. *J Otol*, *12*(3), 117-124. https://doi.org/10.1016/j.joto.2017.06.002

Rachamim, N., Latter, H., Malinin, N., Asher, C., Wald, H., & Garty, H. (1995). Dexamethasone enhances expression of mitochondrial oxidative phosphorylation genes in rat distal colon. *Am J Physiol*, *269*(5 Pt 1), C1305-1310. https://doi.org/10.1152/ajpcell.1995.269.5.C1305

Roca, F. J., & Ramakrishnan, L. (2013). TNF dually mediates resistance and susceptibility to mycobacteria via mitochondrial reactive oxygen species. *Cell*, *153*(3), 521-534. https://doi.org/10.1016/j.cell.2013.03.022

Salt, A. N., Hartsock, J., Plontke, S., LeBel, C., & Piu, F. (2011). Distribution of dexamethasone and preservation of inner ear function following intratympanic delivery of a gel-based formulation. *Audiol Neurootol*, *16*(5), 323-335. https://doi.org/10.1159/000322504

Schneider, C. A., Rasband, W. S., & Eliceiri, K. W. (2012). NIH Image to ImageJ: 25 years of image analysis. *Nat Methods*, *9*(7), 671-675. https://doi.org/10.1038/nmeth.2089

696 Sheets, L., He, X. J., Olt, J., Schreck, M., Petralia, R. S., Wang, Y. X., Zhang, Q., Beirl, A.,
697 Nicolson, T., Marcotti, W., Trapani, J. G., & Kindt, K. S. (2017). Enlargement of Ribbons
698 in Zebrafish Hair Cells Increases Calcium Currents But Disrupts Afferent Spontaneous
699 Activity and Timing of Stimulus Onset. *J Neurosci*, *37*(26), 6299-6313.
700 https://doi.org/10.1523/JNEUROSCI.2878-16.2017
701 Suli, A., Pujol, R., Cunningham, D. E., Hailey, D. W., Prendergast, A., Rubel, E. W., & Raible, D.
702 W. (2016). Innervation regulates synaptic ribbons in lateral line mechanosensory hair
703 cells. *Development*, *143*(12), e1 2. https://doi.org/10.1242/dev.140616
704 Toro, C., Trapani, J. G., Pacentine, I., Maeda, R., Sheets, L., Mo, W., & Nicolson, T. (2015).
705 Dopamine Modulates the Activity of Sensory Hair Cells. *The Journal of neuroscience :*
706 *the official journal of the Society for Neuroscience*, *35*(50), 16494-16503.
707 https://doi.org/10.1523/JNEUROSCI.1691-15.2015
708 Valledor, A. F., & Ricote, M. (2004). Nuclear receptor signaling in macrophages. *Biochem*
709 *Pharmacol*, *67*(2), 201-212. https://doi.org/10.1016/j.bcp.2003.10.016
710 Vettorazzi, S., Nalbantoglu, D., Gebhardt, J. C. M., & Tuckermann, J. (2021). A guide to
711 changing paradigms of glucocorticoid receptor function-a model system for genome
712 regulation and physiology. *FEBS J*. https://doi.org/10.1111/febs.16100
713 Waissbluth, S., Salehi, P., He, X., & Daniel, S. J. (2013). Systemic dexamethasone for the
714 prevention of cisplatin-induced ototoxicity. *Eur Arch Otorhinolaryngol*, *270*(5), 1597-
715 1605. https://doi.org/10.1007/s00405-012-2150-0
716 Warchol, M. E., Schrader, A., & Sheets, L. (2021). Macrophages Respond Rapidly to Ototoxic
717 Injury of Lateral Line Hair Cells but Are Not Required for Hair Cell Regeneration. *Front*
718 *Cell Neurosci*, *14*, 613246. https://doi.org/10.3389/fncel.2020.613246
719 Zhang, Q., Li, S., Wong, H. C., He, X. J., Beirl, A., Petralia, R. S., Wang, Y. X., & Kindt, K. S.
720 (2018). Synaptically silent sensory hair cells in zebrafish are recruited after damage. *Nat*
721 *Commun*, *9*(1), 1388. https://doi.org/10.1038/s41467-018-03806-8

722